

A three-sphere microswimmer in a structured fluid

KENTO YASUDA¹, RYUICHI OKAMOTO² and SHIGEYUKI KOMURA¹

¹ *Department of Chemistry, Graduate School of Science, Tokyo Metropolitan University - Tokyo 192-0397, Japan*

² *Research Institute for Interdisciplinary Science, Okayama University - Okayama 700-8530, Japan*

received 21 May 2018; accepted in final form 27 July 2018

published online 27 August 2018

PACS 47.63.Gd – Swimming microorganisms

PACS 47.63.mf – Low-Reynolds-number motions

PACS 82.70.Gg – Gels and sols

Abstract – We discuss the locomotion of a three-sphere microswimmer in a viscoelastic structured fluid characterized by typical length and time scales. We derive a general expression to link the average swimming velocity to the sphere mobilities. In this relationship, a viscous contribution exists when the time-reversal symmetry is broken, whereas an elastic contribution is present when the structural symmetry of the microswimmer is broken. As an example of a structured fluid, we consider a polymer gel, which is described by a “two-fluid” model. We demonstrate in detail that the competition between the swimmer size and the polymer mesh size gives rise to the rich dynamics of a three-sphere microswimmer.

Copyright © EPLA, 2018

Introduction. – Microswimmers are tiny machines, such as sperm cells or motile bacteria, that swim in a fluid and are expected to be relevant to microfluidics and microsystems [1]. By transforming chemical energy into mechanical work, microswimmers can change their shapes and move in viscous environments. The fluid forces acting on the length scale of microswimmers are governed by the effect of viscous dissipation. According to Purcell’s scallop theorem [2], time-reversal body motion cannot be used for locomotion in a Newtonian fluid. As one of the simplest models exhibiting broken time-reversal symmetry, Najafi and Golestanian proposed a three-sphere microswimmer [3,4] in which three in-line spheres are linked by two arms of varying lengths. This model is suitable for analytical studies because the tensorial structure of the fluid motion can be neglected in its translational motion. Recently, such a microswimmer has been experimentally realized [5,6].

For microswimmers in general situations, however, the surrounding fluid is not necessarily purely viscous but viscoelastic. Several studies have discussed the swimming behaviors of micromachines in different types of viscoelastic fluids [7–11]. In particular, Lauga showed that the Scallop theorem in a viscoelastic fluid breaks down if the squirmer has a fore-aft asymmetry in its surface velocity distribution [7]. In a recent study, we discussed the locomotion of a three-sphere microswimmer in a viscoelastic medium and derived a relationship linking the average swimming velocity to the frequency-dependent viscosity

of the surrounding medium [12]. We demonstrated that the absence of the time-reversal symmetry of the swimmer motion is reflected in the real part of the viscosity, whereas the absence of the structural symmetry of the swimmer is reflected in its imaginary part.

So far, investigations into the swimming behaviors of micromachines have been limited to homogeneous viscoelastic fluids without any internal structures. However, one of the fundamental and characteristic features of viscoelastic soft matter is that it contains various intermediate mesoscopic structures and behaves as a structured fluid [13]. The existence of such internal length scales significantly affects the rheological properties of soft matter [14]. In this letter, we address the effects of the intermediate structures of the surrounding viscoelastic fluid on the locomotion of a three-sphere microswimmer. Because a three-sphere microswimmer is also characterized by its own size, our main interest is to find out how the average swimming velocity depends on the relative magnitudes of the swimmer’s size and the characteristic length of the surrounding fluid.

Generalizing our previous work [12], we first obtain the average velocity of a three-sphere microswimmer moving in a structured fluid, which is characterized by typical length and time scales. As an example of a structured fluid, we employ a “two-fluid” model that has been broadly used to describe the dynamics of polymer gels [15–17]. Recently, the response of a polymer network to the motion of a rigid sphere has been investigated within this two-fluid

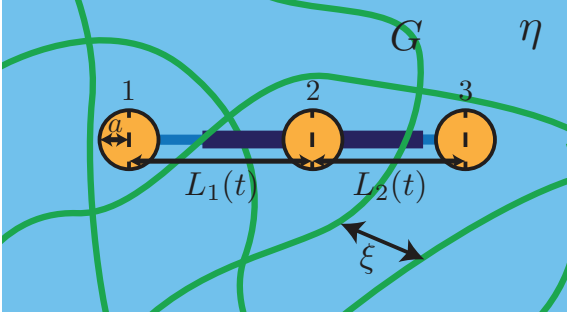


Fig. 1: (Color online) A three-sphere micromachine swimming in a structured fluid such as a polymer gel. Three identical spheres of radius a are connected by arms with lengths $L_1(t)$ and $L_2(t)$ and undergo time-dependent cyclic motions. According to the two-fluid model, the polymer gel consists of an elastic network characterized by a constant shear modulus G and a viscous fluid characterized by a constant shear viscosity η . The elastic and fluid components are coupled via mutual friction. The length scale ξ characterizes the typical internal structure of the elastic network, *e.g.*, its mesh size.

model [18–20]. We calculate the frequency dependence of the average velocity of a three-sphere microswimmer in a two-fluid gel and obtain its various asymptotic expressions by changing the swimmer size. The competition between the swimmer size and the polymer mesh size gives rise to the rich dynamics of microswimmers. Even though we primarily discuss the two-fluid model here, our result can be applied to various types of structured fluids.

Microswimmer in a structured fluid. – As shown in fig. 1, we consider a microswimmer consisting of three rigid spheres of the same radius a that are connected by two arms of variable lengths L_1 and L_2 [3,4]. We assume that the motion of the arms is prescribed by two time-dependent functions $L_1(t), L_2(t) \gg a$. Then the velocity of each sphere V_i ($i = 1, 2, 3$) should satisfy the conditions $\dot{L}_1(t) = V_2(t) - V_1(t)$ and $\dot{L}_2(t) = V_3(t) - V_2(t)$, where the dot indicates the time derivative. The surrounding fluid exerts a force F_i ($i = 1, 2, 3$) on each sphere, which we assume to be along the swimmer axis. Because we are interested in the autonomous net locomotion of the swimmer, there are no external forces acting on the spheres. This leads to the force-free condition: $F_1(t) + F_2(t) + F_3(t) = 0$.

Within the linear response theory, the velocity and force acting on a sphere of radius a are related in the Fourier domain by $V_i(\omega) = \mu[a, \omega]F_i(\omega)$, where $V(\omega) = \int_{-\infty}^{\infty} dt V(t)e^{-i\omega t}$ (with the same form for $F(\omega)$) denotes the Fourier transform and $\mu[a, \omega] = \int_0^{\infty} dt \mu(a, t)e^{-i\omega t}$ gives the frequency-dependent self-mobility. Similarly, the force F_j acting on the j -th sphere at x_j and the induced velocity V_i of the i -th sphere at x_i are related by $V_i(\omega) = M[r, \omega]F_j(\omega)$, where $r = x_i - x_j \gg a$ and $M[r, \omega]$ is the frequency-dependent longitudinal coupling mobility.

We further assume that the arm deformations are relatively small, and given by $L_1(t) = \ell + u_1(t)$ and

$L_2(t) = \ell + u_2(t)$, where ℓ is a constant length that satisfies $\ell \gg u_1(t), u_2(t)$. We consider the case when the two arms undergo the simplest periodic motions [3,4]: $u_1(t) = d_1 \cos(\Omega t)$ and $u_2(t) = d_2 \cos(\Omega t - \phi)$, where d_1 and d_2 are the amplitudes of the oscillatory motions, Ω is the common arm frequency, and ϕ is the mismatch in the phases between the two arms. When the arm motions are given, the above set of equations is sufficient to solve for the six unknown quantities V_i and F_i . The swimming velocity is obtained by averaging the velocities of the three spheres, *i.e.*, $V = (V_1 + V_2 + V_3)/3$.

Consider a viscoelastic structured fluid that is characterized by a characteristic length scale ξ and a characteristic time scale τ . We assume that the above-mentioned mobilities are expressed by the following scaling forms:

$$\mu[a, \omega] = \frac{\hat{\mu}[a/\xi, \omega\tau]}{6\pi\eta_0 a}, \quad M[r, \omega] = \frac{\hat{M}[r/\xi, \omega\tau]}{4\pi\eta_0 \ell}, \quad (1)$$

where $\hat{\mu}$ and \hat{M} are the dimensionless scaling functions and η_0 is the zero-frequency shear viscosity. Even if there are more than two length or time scales, the above assumption is still valid because only the dimensionless ratios between the different scales enter into the scaling functions. In other words, if there are several length scales $\xi_1, \xi_2, \xi_3, \dots$ and several time scales $\tau_1, \tau_2, \tau_3, \dots$, the dimensionless mobility can be expressed as $\hat{\mu}[a/\xi_1, \omega\tau_1; \xi_2/\xi_1, \xi_3/\xi_1, \dots; \tau_2/\tau_1, \tau_3/\tau_1, \dots]$ and similarly for \hat{M} . Under this assumption, we perform an expansion of the swimming velocity to the leading order in $a/\ell, d_1/\ell$, and d_2/ℓ . After performing the time integration over a full cycle, we obtain the average swimming velocity:

see eq. (2) on the next page

where $\partial\hat{M}[\ell/\xi, 0] = \lim_{\omega\tau \rightarrow 0} (\partial\hat{M}[r/\xi, \omega\tau]/\partial r)_{r=\ell}$ (see the Supplementary Material [Supplementarymaterial.pdf](#) (SM) for the full derivation). This is a generalization of our previous result [12] and is the main result of this letter.

The first term in eq. (2) can be regarded as a viscous contribution, \bar{V}_v , and is present only if the time-reversal symmetry of the arm motion is broken, *i.e.*, $\phi \neq 0, \pi$. The second term, conversely, corresponds to an elastic contribution, \bar{V}_e , and exists only when the structural symmetry of the swimmer is broken, *i.e.*, $d_1 \neq d_2$. In other words, even if the time-reversal symmetry of the swimmer motion is not broken, *i.e.*, $\phi = 0, \pi$, the swimmer can still move in a viscoelastic medium because of the second elastic term as long as its structural symmetry is broken, *i.e.*, $d_1 \neq d_2$. We used the condition $a \ll \ell$ when deriving eq. (2), but nothing has been assumed concerning the relative magnitudes between the swimmer size, a and ℓ , and the characteristic length of the fluid, ξ . Therefore, eq. (2) offers a very general velocity expression for a three-sphere microswimmer moving in a structured fluid.

Although eq. (2) is applicable to any structured fluid, some special cases are worth discussing. For a purely viscous fluid, the scaling functions in eq. (1) are given by

$$\begin{aligned} \bar{\mathbf{V}} \approx & \frac{d_1 d_2 a \Omega}{48 \ell^2} (\hat{\mu}[a/\xi, \Omega\tau]^{-1} + \hat{\mu}[a/\xi, -\Omega\tau]^{-1}) \left(8\hat{M}[\ell/\xi, 0] - \hat{M}[2\ell/\xi, 0] + 2\ell(-4\partial\hat{M}[\ell/\xi, 0] + \partial\hat{M}[2\ell/\xi, 0]) \right) \sin\phi \\ & + \frac{i(d_1^2 - d_2^2)a\Omega}{96\ell^2} (\hat{\mu}[a/\xi, \Omega\tau]^{-1} - \hat{\mu}[a/\xi, -\Omega\tau]^{-1}) \left(4\hat{M}[\ell/\xi, 0] + \hat{M}[2\ell/\xi, 0] - 2\ell(2\partial\hat{M}[\ell/\xi, 0] + \partial\hat{M}[2\ell/\xi, 0]) \right), \quad (2) \end{aligned}$$

$\hat{\mu} = 1$ and $\hat{M} = 1$; therefore, eq. (2) reduces to the average velocity obtained by Golestanian and Ajdari [4]. Further, for a viscoelastic fluid without any internal structure, the scaling functions are simply given by $\hat{\mu} = \eta_0/\eta[\omega]$ and $\hat{M} = \eta_0/\eta[\omega]$, where $\eta[\omega]$ is the frequency-dependent complex viscosity. In such a homogeneous but viscoelastic fluid, eq. (2) reduces to eq. (13) in ref. [12].

We note that the above derivation has been limited within the linear response theory because linear relationships between forces and velocities have been assumed. Such an assumption of the linear viscoelasticity is generally justified when the strain amplitude is small enough [21]. For a three-sphere microswimmer, this condition is given by $d_1/\ell \ll 1$ and $d_2/\ell \ll 1$ which have been indeed used in the derivation of eq. (2). Otherwise, one needs to take into account nonlinear viscoelastic effects such as a shear-thinning behavior [14].

Two-fluid model for a gel. – As a simple example of various structured fluids, we consider here a polymer gel described by the two-fluid model. As schematically described in fig. 1, there are two dynamical fields in this model: the displacement field $\mathbf{u}(\mathbf{r}, t)$ of the elastic network and the velocity field $\mathbf{v}(\mathbf{r}, t)$ of the permeating fluid. When inertial effects are neglected, the linearized coupled equations for these two field variables are given by

$$0 = G\nabla^2 \mathbf{u} + (K + G/3)\nabla(\nabla \cdot \mathbf{u}) - \Gamma \left(\frac{\partial \mathbf{u}}{\partial t} - \mathbf{v} \right), \quad (3)$$

$$0 = \eta\nabla^2 \mathbf{v} - \nabla p - \Gamma \left(\mathbf{v} - \frac{\partial \mathbf{u}}{\partial t} \right) + \mathbf{f}. \quad (4)$$

Here, G and K are the shear and compression moduli of the elastic network, respectively, η is the shear viscosity of the fluid, $p(\mathbf{r}, t)$ is the pressure field, and $\mathbf{f}(\mathbf{r}, t)$ is the external force density acting on the fluid component. The elastic and fluid components are coupled via the mutual friction, which is characterized by the friction coefficient Γ . When the volume fraction of the elastic component is small, we further require the incompressibility condition: $\nabla \cdot \mathbf{v} = 0$. The above two-fluid model contains the characteristic length $\xi = (\eta/\Gamma)^{1/2}$ and the characteristic time $\tau = \eta/G$. The former length scale roughly corresponds to the mesh size of a polymer network, and the latter time scale sets the viscoelastic time. Hereafter, we introduce a dimensionless ratio defined as $\epsilon = [(K + 4G/3)/G]^{1/2}$.

Diamant calculated the self-mobility of a sphere in a two-fluid gel, which depends on the choice of the boundary condition at the surface of the sphere [18]. Here we consider the case of “a sticking fluid and a free network”, *i.e.*,

a stick boundary condition is used for the fluid while the network does not exchange stress with the sphere. In other words, the network moves only because of its coupling to the fluid. The full expression of the self-mobility μ is given in the SM [18], and here we show only its limiting behaviors. In the low-frequency limit, $\omega\tau \rightarrow 0$, μ becomes

$$\begin{aligned} \mu[a, \omega] \approx & \frac{9}{6\pi\eta a(9 + 9\hat{a} + \hat{a}^2)} \\ & + \frac{i\omega\tau}{6\pi\eta\xi} \frac{(4 + 3\epsilon^2)\hat{a}^3 + 36\epsilon^2\hat{a}^2 + 162\epsilon^2\hat{a} + 81\epsilon^2}{2(9 + 9\hat{a} + \hat{a}^2)^2\epsilon^2}, \quad (5) \end{aligned}$$

where $\hat{a} = a/\xi$ and one can take further limits depending on the magnitude of \hat{a} . In the high-frequency limit, $\omega\tau \rightarrow \infty$, μ becomes

$$\mu[a, \omega] \approx \frac{1}{6\pi\eta a} - \frac{1}{6\pi\eta a(i\omega\tau)}. \quad (6)$$

This expression is equivalent to writing the mobility as $\mu[a, \omega] \approx 1/(6\pi\eta_b a)$, with an effective viscosity of $\eta_b = \eta[1 + 1/(i\omega\tau)]$. Therefore, the above two-fluid model reduces to the Kelvin-Voigt model at high frequencies [14].

We previously obtained a general expression for the coupling mobility M connecting the velocity \mathbf{v} and the force \mathbf{f} in the two-fluid model [22,23], which is also given in the SM. For small distances, $r/\xi \rightarrow 0$, the coupling mobility is

$$M[r, \omega] \approx \frac{1}{4\pi\eta r} - \frac{1}{6\pi\eta\xi(1 + i\omega\tau)^{1/2}}, \quad (7)$$

and consequently, the gel is nearly purely viscous. Conversely, for sufficiently large distances, $r/\xi \rightarrow \infty$, the coupling mobility is

$$M[r, \omega] \approx \frac{1}{4\pi\eta_b r} + \frac{\xi^2}{2\pi\eta r^3} \frac{1}{(1 + i\omega\tau)^2}. \quad (8)$$

Average velocities in a two-fluid gel. – Next we discuss the average velocity of a three-sphere microswimmer in a two-fluid gel and investigate its frequency as well as size dependences. Recall that there are two lengths that measure the size of a three-sphere microswimmer: the sphere radius a and the average arm length ℓ , with the condition $a \ll \ell$. Because the surrounding gel is characterized by the network mesh size, ξ , the following three different situations can be distinguished: i) a large swimmer when $a \gg \xi$ and $\ell \gg \xi$, ii) a medium swimmer when $a \ll \xi$ and $\ell \gg \xi$, and iii) a small swimmer when $a \ll \xi$ and $\ell \ll \xi$. In each case, following the procedure in the SM, we numerically solve for V_i and F_i to calculate the

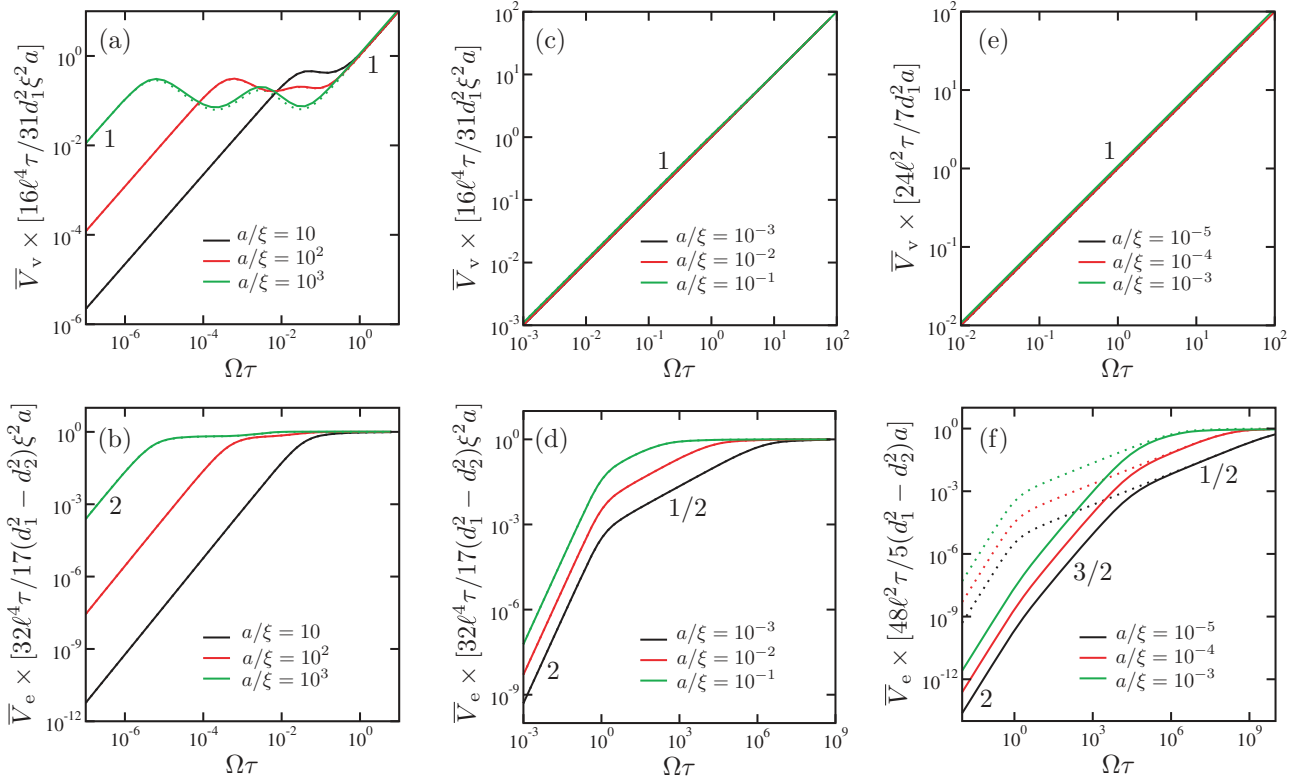


Fig. 2: (Color online) Plots of the average swimming velocity \bar{V} as a function of the scaled frequency $\Omega\tau$ for a three-sphere micromachine swimming in a polymer gel with $\epsilon = [(K + 4G/3)/G]^{1/2} = \sqrt{14/3} \approx 2.16$. The solid lines are the numerical results explained in the text, whereas the dotted lines (with the same colors) are the analytical results obtained from eq. (2). The analytical dotted curves are invisible when they coincide with the numerical solid curves. The numbers indicate the slopes representing the exponents of the power-law behaviors. (a) The scaled viscous contribution \bar{V}_v and (b) the scaled elastic contribution \bar{V}_e for a large swimmer ($a \gg \xi, \ell \gg \xi$). The different colors correspond to the different a/ξ values shown in the graphs; here, we have chosen $\ell/\xi = 10^4$. The other parameters are $\phi = \pi/2$ and $d_1/\ell = d_2/\ell = 10^{-2}$ in (a) and $d_1 = 2d_2$ and $d_2/\ell = 10^{-2}$ in (b). (c) The scaled \bar{V}_v and (d) scaled \bar{V}_e for a medium swimmer ($a \ll \xi, \ell \gg \xi$). The different colors correspond to the different a/ξ values shown in the graphs; here, we have chosen $\ell/\xi = 10^4$. The other parameters are the same as those in (a) and (b). (e) The scaled \bar{V}_v and (d) scaled \bar{V}_e for a small swimmer ($a \ll \xi, \ell \ll \xi$). The different colors correspond to the different a/ξ values shown in the graphs; here, we have chosen $\ell/\xi = 10^{-2}$. The other parameters are the same as those in (a) and (b). Notice that in all these plots, a/ξ and ℓ/ξ are chosen in such a way that $a/\ell \ll 1$ is always satisfied.

average velocity \bar{V} without making an expansion in terms of a/ℓ . These numerical results are plotted by the solid lines in fig. 2, whereas the analytical results obtained from eq. (2) are plotted by the dotted lines with the same colors. In fig. 2, the parameters a/ξ and ℓ/ξ are chosen in such a way that the condition $a/\ell \ll 1$ is always satisfied for a three-sphere microswimmer. Moreover, d_1/ℓ and d_2/ℓ are also small enough to ensure that the assumption of linear viscoelasticity is appropriate.

In figs. 2(a) and (b), we separately plot the viscous \bar{V}_v and elastic \bar{V}_e contributions, respectively, for a large swimmer as a function of the scaled frequency $\Omega\tau$. The behavior of \bar{V}_v in fig. 2(a) is remarkable because it exhibits a non-monotonic dependence on Ω . A careful analysis reveals that it behaves as $\bar{V}_v \sim \Omega \rightarrow \Omega^{-1/2} \rightarrow \Omega \rightarrow \Omega^{-1} \rightarrow \Omega$ as Ω increases. This non-monotonic behavior is more pronounced for larger sphere sizes such as $a/\xi = 100$ (green). On the other hand, the frequency dependence of the elastic contribution, \bar{V}_e , crosses over as $\bar{V}_e \sim \Omega^2 \rightarrow \Omega^0$.

The above results can be reproduced by eq. (2) when we use the full expressions of the two-fluid mobilities μ and M (most of the dotted lines in fig. 2 are invisible because they almost coincide with the solid lines). Further, eq. (2) provides us with various asymptotic expressions. For example, we first discuss the limit of $\Omega\tau \rightarrow 0$ in \bar{V}_v . Using the first term of eq. (5) and the second term of eq. (8), we obtain

$$\bar{V}_v \approx \frac{31d_1d_2a^3\Omega}{144\ell^4} \sin \phi, \quad (9)$$

which is proportional to Ω . The complex non-monotonic behaviors in the intermediate frequencies are separately discussed in the SM. In the limit of $\Omega\tau \rightarrow \infty$, we use the first term of eq. (6) and the second term of eq. (8) to obtain

$$\bar{V}_v \approx \frac{31d_1d_2\xi^2a\Omega}{16\ell^4} \sin \phi. \quad (10)$$

By evaluating the elastic term in eq. (2), one can also obtain the asymptotic expressions for \bar{V}_e . In the limit of

$\Omega\tau \rightarrow 0$, we use the second terms of eqs. (5) and (8) to obtain

$$\bar{V}_e \approx \frac{17(d_1^2 - d_2^2)a^5}{5184\ell^4\xi^2\tau} \frac{4 + 3\epsilon^2}{\epsilon^2} (\Omega\tau)^2, \quad (11)$$

which is proportional to Ω^2 . In the limit of $\Omega\tau \rightarrow \infty$, the second terms of eqs. (6) and (8) yield

$$\bar{V}_e \approx \frac{17(d_1^2 - d_2^2)\xi^2 a}{32\ell^4\tau}, \quad (12)$$

which is independent of Ω . Notice that the crossover frequency separating the different scaling regimes is strongly dependent on a/ξ . For example, the crossover frequency between eqs. (11) and (12) roughly scales as $(\Omega\tau)^* \sim (a/\xi)^{-2}$. This means that one can extract information concerning the internal structure of the surrounding medium by observing the average swimming velocity. Moreover, the non-linear dependence on the sphere size, such as $\bar{V}_v \sim a^3$ in eq. (9) or $\bar{V}_e \sim a^5$ in eq. (11), is also a unique feature of a two-fluid gel.

For a medium swimmer ($a \ll \xi$ and $\ell \gg \xi$), we plot the numerical results of \bar{V}_v and \bar{V}_e in figs. 2(c) and (d), respectively. In fig. 2(c), we find $\bar{V}_v \sim \Omega$ over the entire frequency range. This behavior is essentially explained by eq. (10), which was obtained for the large swimmer case. The elastic contribution in fig. 2(d), conversely, crosses over as $\bar{V}_e \sim \Omega^2 \rightarrow \Omega^{1/2} \rightarrow \Omega^0$, where the Ω -independent behavior can be explained by eq. (12) as before. In the SM, we show the asymptotic expressions for smaller frequencies (see eqs. (S40) and (S41)).

Finally, we numerically plot \bar{V}_v and \bar{V}_e for a small swimmer ($a \ll \xi$ and $\ell \ll \xi$) in figs. 2(e) and (f), respectively. The viscous contribution shows a linear dependence, $\bar{V}_v \sim \Omega$. This is reasonable because the combination of the first terms in eqs. (6) and (7) simply represents a purely viscous fluid. The elastic contribution plotted in fig. 2(f) crosses over as $\bar{V}_e \sim \Omega^2 \rightarrow \Omega^{3/2} \rightarrow \Omega^{1/2} \rightarrow \Omega^0$. Even though the first two scaling behaviors cannot be obtained analytically, the last two behaviors are given in the SM (see eqs. (S42) and (S43)). It should be mentioned here that eq. (2) does not reproduce the numerical result in fig. 2(f) because the lowest expansion in terms of a/ℓ is inappropriate for this limit. Hence the dotted lines deviate from the solid lines fig. 2(f) especially for relatively smaller $\Omega\tau$ values.

Discussion. – So far, we have primarily discussed the motion of a three-sphere microswimmer in a polymer gel described by the two-fluid model. However, the importance of our work is not restricted to these specific models. The prediction of the average velocity in eq. (2) is applicable to any structured viscoelastic fluid that has an intermediate length scale and a characteristic time scale. For example, one can also discuss the motion of a microswimmer in a polymer solution that is described by a different “two-fluid” model [24,25]. In addition, it is interesting to discuss the dynamics of three-sphere microswimmers in

liquid crystals [26], which typically exhibit complex rheological behavior depending on their different phases [27].

Furthermore, we encounter a similar situation when we consider the motion of a three-disk microswimmer immersed in a quasi-2D fluid membrane [28]. Owing to the presence of the hydrodynamic screening length in the quasi-2D fluid, the geometric factor appearing in the average velocity exhibits various asymptotic behaviors when changing the ratio between the swimmer size and the screening length. The result in ref. [28] can be obtained from eq. (2) using the mobility of the disk and the coupling mobility in a quasi-2D fluid.

At this point, it is useful to give some numbers related to realistic microswimmers and systems described by a two-fluid model. Let us first consider a homogeneous sample of entangled F-actin network whose mesh size ξ can be controlled by the actin monomer concentration c as $\xi = 0.3/\sqrt{c}$ (ξ in μm and c in mg/ml) [19,20]. Hence $\xi \approx 1\mu\text{m}$ for $c \approx 0.1\text{mg/ml}$. On the other hand, a typical size of colloidal particles used in microrheology experiments is $a \approx 0.5\mu\text{m}$ [29]. If we assume that one can construct a three-sphere microswimmer by connecting these colloidal particles, its whole size (corresponding to ℓ) would amount to several microns, which is comparable to a typical size of living microorganisms such as bacteria. Since a magnitude relation $a < \xi < \ell$ holds in this case, a living microorganism swimming in an actin network may correspond to a medium swimmer (see fig. 2(c) and (d)).

On the other hand, a three-sphere swimmer has been experimentally realized by using ferromagnetic particles at an air-water interface and by applying an oscillating magnetic field [5,6]. In this experiment, the size of spheres is about $a \approx 200\mu\text{m}$ and the rest length of the bonds is roughly $\ell \approx 1\text{mm}$. Hence such a model swimmer behaves as a large swimmer in an actin network (see fig. 2(a) and (b)), since the mesh size is much smaller, *i.e.*, $\xi \ll a < \ell$. Such a comparison shows that the swimming behaviors of a microorganism and a ferromagnetic swimmer are essentially different in a structured fluid such as F-actin networks due to the presence of the characteristic length scale ξ . This is the main message of the present work.

Concerning the characteristic time scale τ of a two-fluid model, we shall refer to a number that was measured for F-actin networks [19,20] by using microrheology techniques [29]. With the water viscosity $\eta \approx 10^{-3}\text{Pa}\cdot\text{s}$ and the measured shear modulus $G \approx 10^{-1}\text{Pa}$ for a F-actin network, we obtain the viscoelastic time scale as $\tau = \eta/G \approx 10^{-2}\text{s}$. For a typical microorganism and a model swimmer mentioned above, characteristic frequencies are about $\Omega \approx 10^2\text{Hz}$ [1] and 1Hz [5,6], respectively. Hence the corresponding Deborah numbers $\text{De} = \Omega\tau$ for these two cases are $\text{De} \approx 1$ (microorganism) and 10^{-2} (model swimmer) which are both considered in fig. 2.

Finally, we note that Fu *et al.* analyzed the swimming behavior of an infinite sheet undergoing transverse traveling-wave deformations in a two-fluid gel [30].

They demonstrated that the boundary conditions between the sheet and the network significantly affect the swimming speed. In our study, we considered only the case of “a sticking fluid and a free network” for the boundary condition between the sphere and the gel. Different situations such as “a sticking fluid and a sticking network” case or “a sticking fluid and a slipping network” case, as discussed in detail in ref. [18], will lead to different swimming behaviors because the self-mobility of the spheres is modified. Although several deficiencies of the two-fluid model have been explicitly pointed out [18], such investigations are left to future studies.

Summary. – We discussed the locomotion of a three-sphere microswimmer in a viscoelastic structured fluid with typical length and time scales. We derived a general expression for the average swimming velocity, eq. (2), which includes both viscous and elastic contributions. To illustrate our result, we used the two-fluid model for a polymer gel and demonstrated that the average velocity exhibits various asymptotic behaviors depending on the swimmer size. Because one can extract information concerning the internal structure of the surrounding fluid from observations of the motion of a microswimmer, the present theory offers a new approach to active microrheology [29].

* * *

KY acknowledges support by a Grant-in-Aid for JSPS Fellows (Grant No. 18J21231) from the Japan Society for the Promotion of Science (JSPS). SK acknowledges support by a Grant-in-Aid for Scientific Research (C) (Grant No. 18K03567) from the JSPS.

REFERENCES

- [1] LAUGA E. and POWERS T. R., *Rep. Prog. Phys.*, **72** (2009) 096601.
- [2] PURCELL E. M., *Am. J. Phys.*, **45** (1977) 3.
- [3] NAJAFI A. and GOLESTANIAN R., *Phys. Rev. E*, **69** (2004) 062901.
- [4] GOLESTANIAN R. and AJDARI A., *Phys. Rev. E*, **77** (2008) 036308.
- [5] GROSJEAN G., HUBERT M., LAGUBEAU G. and VANDEWALLE N., *Phys. Rev. E*, **94** (2016) 021101(R).
- [6] GROSJEAN G., HUBERT M. and VANDEWALLE N., *Adv. Colloid Interface Sci.*, **255** (2018) 84.
- [7] LAUGA E., *EPL*, **86** (2009) 64001.
- [8] TERAN J., FAUCI L. and SHELLEY M., *Phys. Rev. Lett.*, **104** (2010) 038101.
- [9] CURTIS M. P. and GAFFNEY E. A., *Phys. Rev. E*, **87** (2013) 043006.
- [10] QIU T., LEE T.-C., MARK A. G., MOROZOV K. I., MUNSTER R., MIERKA O., TUREK S., LESHANSKY A. M. and FISCHER P., *Nat. Commun.*, **5** (2014) 5119.
- [11] ISHIMOTO K. and GAFFNEY E. A., *J. Fluid Mech.*, **831** (2017) 228.
- [12] YASUDA K., OKAMOTO R. and KOMURA S., *J. Phys. Soc. Jpn.*, **86** (2017) 043801.
- [13] WITTEN T. A. and PINCUS P., *Structured Fluids* (Oxford University Press, Oxford) 2004.
- [14] LARSON R. G., *The Structure and Rheology of Complex Fluids* (Oxford University Press, Oxford) 1999.
- [15] DE GENNES P. G., *Macromolecules*, **9** (1976) 587.
- [16] DE GENNES P. G., *Macromolecules*, **9** (1976) 594.
- [17] BROCHARD F. and DE GENNES P. G., *Macromolecules*, **10** (1977) 1157.
- [18] DIAMANT H., *Eur. Phys. J. E*, **38** (2015) 32.
- [19] SONN-SEGEV A., BERNHEIM-GROSWASSER A., DIAMANT H. and ROICHMAN Y., *Phys. Rev. Lett.*, **112** (2014) 088301.
- [20] SONN-SEGEV A., BERNHEIM-GROSWASSER A. and ROICHMAN Y., *Soft Matter*, **10** (2014) 8324.
- [21] PIPKIN A. C., *Lectures on Viscoelasticity Theory* (Springer-Verlag, New York) 1972.
- [22] YASUDA K., OKAMOTO R., KOMURA S. and MIKHAILOV A. S., *EPL*, **117** (2017) 38001.
- [23] YASUDA K., OKAMOTO R. and KOMURA S., *Phys. Rev. E*, **95** (2017) 032417.
- [24] DOI M. and ONUKI A., *J. Phys. II*, **2** (1992) 1631.
- [25] BRUINSMA R., GROSBURG A. Y., RABIN Y. and ZIDOVSKA A., *Biophys. J.*, **106** (2014) 1871.
- [26] KRIEGER M. S., SPAGNOLIEB S. E. and POWERS T., *Soft Matter*, **11** (2015) 9115.
- [27] FUJII S., KOMURA S. and LU C.-Y. D., *Materials*, **7** (2014) 5146.
- [28] OTA Y., HOSAKA Y., YASUDA K. and KOMURA S., *Phys. Rev. E*, **97** (2018) 052612.
- [29] FURST E. M. and SQUIRES T. M., *Microrheology* (Oxford University Press, Oxford) 2017.
- [30] FU H. C., SHENOY V. B. and POWERS T. R., *EPL*, **91** (2010) 24002.